

# Highly Photosensitive Surface Relief Gratings Formation in a Liquid Crystalline Azobenzene Polymer: New Implications for the Migration Process

Nobuyuki Zettsu,<sup>‡</sup> Toshinobu Ogasawara,<sup>†</sup> Ryusuke Arakawa,<sup>†</sup> Susaku Nagano,<sup>†</sup> Takashi Ubukata,<sup>§</sup> and Takahiro Seki<sup>\*,†</sup>

Department of Molecular Design and Engineering, Graduate School of Engineering, Nagoya University, Chikusa, Nagoya 464-8603, Japan; Research Center for Ultra-Precision Science and Technology, Graduate School of Engineering, Osaka University, Yamadaoka, Suita Osaka 565-0871, Japan; and Department of Graduate School of Engineering, Yokohama National University, Tokiwadai, Hodogaya, Yokohama 240-8501, Japan

Received March 16, 2007; Revised Manuscript Received April 26, 2007

**ABSTRACT:** We have recently demonstrated a markedly photosensitive surface relief gratings (SRG) formation in thin films of liquid crystalline azobenzene-containing polymers, which proceeds from a cis-rich state of the azobenzene [Zettsu et al. *Adv. Mater.* **2001**, *13*, 1693; *Macromolecules* **2004**, *37*, 8692]. Such polymers exhibited unexpected enhancements in the sensitivity to light for the completion of SRG formation, the required energy dose being  $\sim 10^3$ -fold lower than that for other azobenzene polymers systems widely employed. Here we report detailed results on the systematic explorations for understanding the migration mechanism. The cis-isomer content at the initial state and irradiation intensity crucially influenced the migration efficiency and the resulting relief structure in nonlinear manners. The Zisman plot showed that the light irradiation leads to a large change in the critical surface tension. Such results strongly suggest that the photochemically induced phase transition and the resulting spatial modulations in the physical properties in the film play the essential roles for the SRG formation. On the basis of this knowledge, the SRG formation via a sensitized excitation was demonstrated for the first time by incorporation of a near-infrared absorbing dye.

## Introduction

Azobenzene derivatives undergo the  $\text{trans} \rightleftharpoons \text{cis}$  photoisomerization under light irradiation. This structural alternation at the molecule level can be transformed to dynamic motions with more than micrometer levels under appropriate reaction fields and light irradiation conditions.<sup>1</sup> The photoisomerization in the nematic liquid crystals, for instance, results in isothermal phase transition from a liquid crystal state to an isotropic liquid phase.<sup>2,3</sup> This phase transition can be repeated over 1000 times by alternate irradiation with ultraviolet (UV) and visible light. The shape difference between the *trans*- and *cis*-azobenzene isomers significantly affects the molecular organization. The former state promotes the liquid crystalline state, and the latter destroys it. Thus, the reversible  $\text{cis} \rightleftharpoons \text{trans}$  photoisomerization acts as the trigger to disrupt or restore the ordered molecular organization.<sup>2–4</sup>

On the other hand, since the first report by Natanshon's and Tripathy's research groups in 1995,<sup>5,6</sup> the formation of photo-induced surface relief gratings (SRG) has recently been attracting considerable attention due to both their potential utility for optical applications and academic interests.<sup>7,8</sup> Exposing an amorphous azobenzene polymer film to the interference pattern of an argon ion ( $\text{Ar}^+$ ) laser beam results in formation of sinusoidal undulations on the film. The topological structure, corresponding to the interference periodicity of the light, can be reversibly erased and rewritten by heating up above the glass transition temperature of the polymer and the subsequent holographic illumination, respectively. Despite accumulated

experimental and theoretical efforts to elucidate the origin of material transfer, the phenomena are not yet fully understood.<sup>9</sup> The characteristic of SRG formation seems to be strongly dependent on numerous experimental parameters involving the features of materials used and the mode and conditions of light irradiation.

A number of amorphous polymers were used for the SRG study, but liquid crystalline polymers are also alluring candidates for the SRG formation.<sup>10–13</sup> There seems to be a couple of significant differences between the amorphous and liquid crystalline polymers. Ramanujam's group have investigated the SRG formation of liquid crystalline polyesters possessing azobenzene derivatives with different substituents.<sup>14</sup> They showed that the SRG formation can be observed only when the experiments are carried out around the glass transition temperature ( $T_g$ ) of a narrow range, implying that the photochemical change in the physical properties of the polymer film should be coupled with the effective mass migration. We have recently developed a family of liquid crystalline azobenzene polymers applicable for SRG formation.<sup>15–19</sup> Unexpectedly large enhancement is observed with respect to the sensitivity required for the SRG formation, i.e., the photon dose required for the completion of migration being  $\sim 10^3$ -fold lower than that for the widely reported amorphous and liquid crystalline polymers. In these systems, preexposure of the films to ultraviolet (UV) light was essential for the enhancement of photosensitivity, and this effect is observed only for azobenzene polymers exhibiting a liquid crystal phase at the ambient temperature. However, there remain many issues to be solved for this phenomenon.

In this work, systematic explorations are made to shed light on the mechanism of migration, especially focusing on the correlation between the content of photoisomers and the

\* Corresponding author. E-mail: tseki@apchem.nagoya-u.ac.jp.

<sup>†</sup> Nagoya University.

<sup>‡</sup> Osaka University.

<sup>§</sup> Yokohama National University.



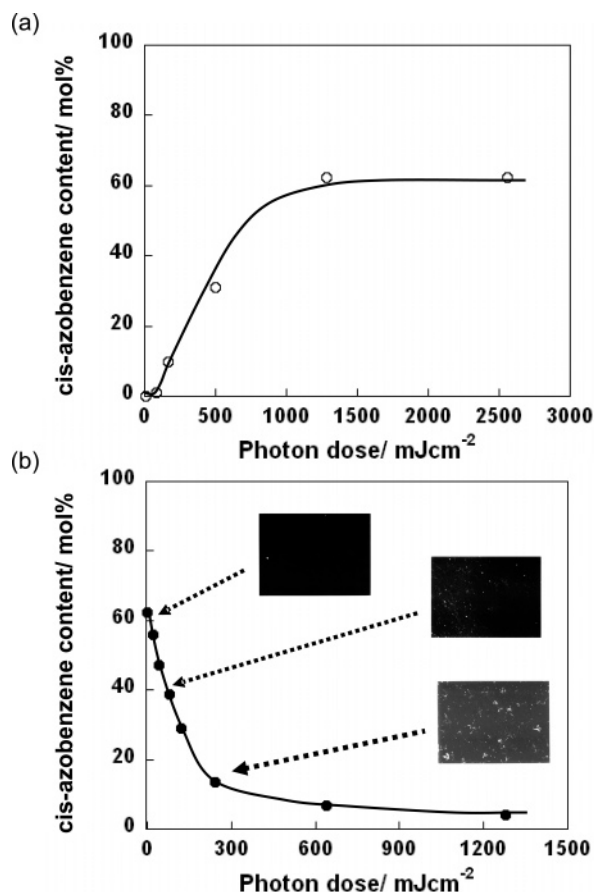


**Figure 2.** Changes in the content of *cis*-azobenzene as a function of exposure energy with irradiation at 365 nm UV light (a) and subsequent 436 nm blue light (b).

The low efficiency of the *trans*-to-*cis* photoisomerization should be attributed to both formation of H-aggregation and highly vertical orientation of the azobenzene chromophore that decreases the probability of light absorption. The content of the *cis*-azobenzene estimated by eq 1 was 60–70% at the photostationary state (Figure 2a). In contrast, the fraction of *cis*-isomer in the film at the photostationary state is considerably lower than that in solution (cf. 95% in solution). Subsequent 436 nm light irradiation to the film reduced the fraction to ~5% (Figure 2b), which was significantly lower than that in solution (30%). It is meaningful to note that the recovered *trans*-isomer become photochemically inactive under subsequent visible light irradiation, which is probably due to the simultaneous rapid self-assembly to form the H-aggregate and the induction of vertical orientation.

We further confirmed that the photochemical phase transition<sup>2,3</sup> actually occurred in the same film of ~600 nm thickness. Using this thicker film, direct optical observation of the phase transition became possible by the polarized optical microscopy (insets in Figure 2b). The phase transition between the liquid crystal and the isotropic liquid phases took place in the film upon photoirradiation with UV light. It was found here that the *cis*-isomer fraction required for the photoinduced phase transition was above 40%. The reverse phase transition occurred when the blue light was illuminated. In contrast, no phase transition was observed below this content. The photoinduced phase transition governed by the *cis* content should be strongly coupled with the SRG formation behavior as mentioned below.

**Effects of Initial *Cis*-Isomer Content on the SRG Formation.** We assumed that the photochemical phase transition as

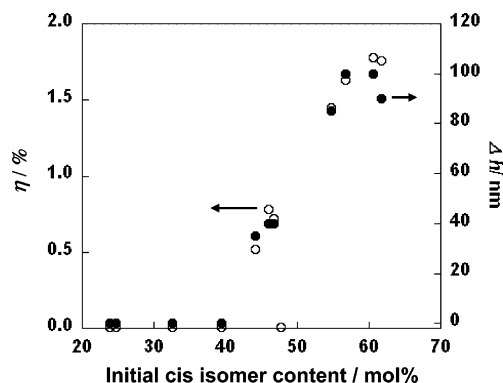


**Figure 3.** Mass migration behavior starting from the p6Az10Ac-PE4.5-(50) films with varied *cis*-isomer content: Data of the first-order diffraction efficiency  $\eta$  (open circle) and surface modulation depth  $\Delta h$  (closed circle) are displayed. SRG formation was achieved under common irradiation energy of 100 mJ cm<sup>-2</sup> for all samples.

described above is closely related to the highly efficient SRG formation. To confirm this, we systematically varied the *cis*-azobenzene isomer content at the initial state by changing the pre-UV exposure doses before the holographic irradiation. Figure 3 depicts the maximum level of the first-order diffraction efficiency  $\eta$  (open circle) and the surface modulation depth (top-to-valley depth)  $\Delta h$  (closed circle) for the p6Az10Ac-PE4.5-(50) film as a function of the initial *cis*-isomer contents. Clearly, the resultant  $\eta$  and  $\Delta h$  strongly depended on the initial *cis*-azobenzene content. The plots of  $\eta$  and  $\Delta h$  fall on a same profile, indicating that the increase in the diffraction efficiency is originated from the formation of SRG (mass migration). Below 40% of the *cis* content, essentially no mass migration occurred. Above this criterion level, the efficiency sharply enhanced to give a saturated efficiency around 60% of the *cis* content. By comparison with the data in Figure 2, it is concluded that the mass migration proceeds only when the interference irradiation is achieved from the isotropic liquid state at the initial. In other words, the cooperative molecular motions taking place during the isotropic to liquid crystal phase transition play an essential role in the highly efficient lateral mass transfer. This can be the most characteristic feature of the present process.

**Effects of Irradiation Intensity on the SRG Formation.** Generally, the variation of light intensity varies only the photochemical reaction rate. However, in molecular assembly systems, nonlinear phenomena can be involved with respect to the irradiation light intensity. In this context, the intensity of the interference beam of Ar<sup>+</sup> laser was changed from 0.1 to 10 mW cm<sup>-2</sup>. Figure 4a shows profiles of the enhancement of the first-order diffraction intensity as a function of exposure time with varied intensities in the holographic irradiation starting from the isotropic state. As clearly indicated, the slope of the increase of diffraction intensity became steeper as the laser intensity was increased. This result implies that the rate of mass transfer monotonously enhances with increase of the laser intensity. The saturated level of diffraction efficiency, on the other hand, varied in different manners.

The final diffraction efficiency  $\eta$  (open circle) and surface modulation (top-to-valley) depth  $\Delta h$  (closed circle) obtained with different writing laser intensity are summarized in Figure 4b. Here, the total photon dose was fixed at 100 mJ cm<sup>-2</sup> in all cases. For all series of data, the maximum value of  $\eta$  (1.7%) and the largest  $\Delta h$  (120 nm) were obtained at a moderate intensity of 2.0 mW cm<sup>-2</sup>. These values decreased at both higher and lower laser intensities. The cross-sectional analysis of the resulting inscriptions evaluated by AFM is shown in Figure 4c.



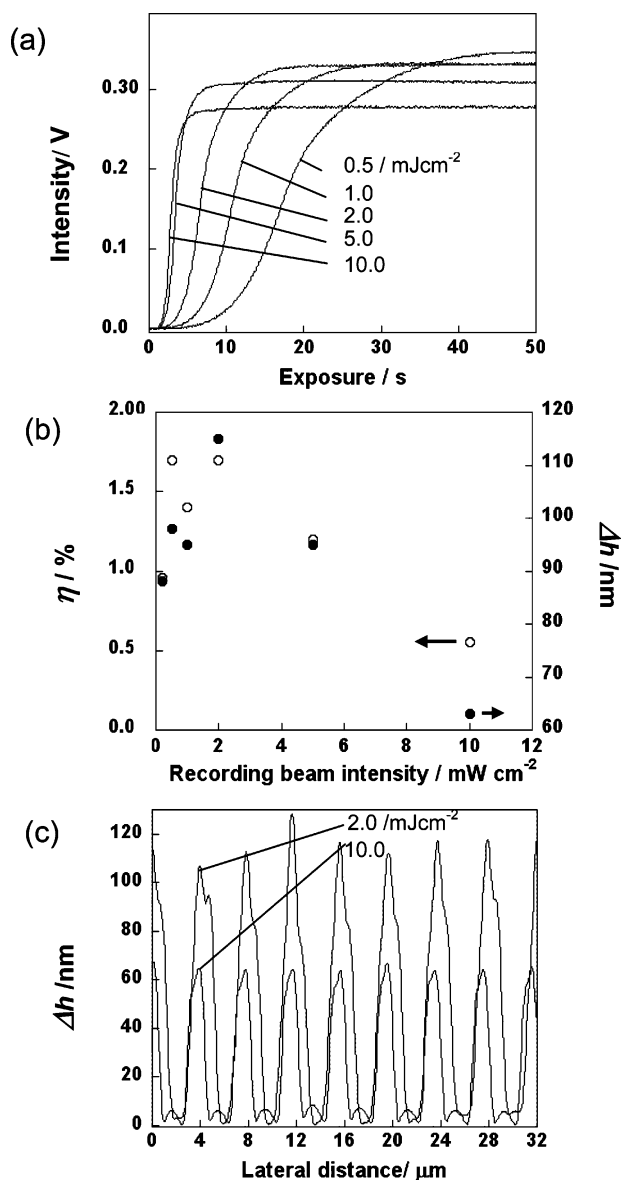


**Figure 4.** Effect of irradiation intensity of the  $\text{Ar}^+$  laser on the relief formation. The intensity was systematically varied to 0.1 to 10  $\text{mW cm}^{-2}$ . (a) Changes in the diffraction intensity as a function of exposure time. (b) The resulting first-order diffraction efficiency  $\eta$  and surface modulation depth  $\Delta h$  after the holographic irradiation at 100  $\text{mJ cm}^{-2}$  in all cases. (c) Cross-sectional height profiles of the SRG structures prepared at 2 or 10  $\text{mW cm}^{-2}$  (total photon dose: 100  $\text{mJ cm}^{-2}$ ).

At 2.0  $\text{mW cm}^{-2}$ , the depth modulations of ca. 120 nm were fabricated from a flat film of 50 nm thickness. This means that almost full migration occurred to a level where the bare substrate surface was exposed. In contrast, the mass transfer ceased at an incomplete stage when irradiation was performed at 10  $\text{mW cm}^{-2}$ , judging from the considerable smaller  $\Delta h$ . The existence of the optimum light intensity for the SRG formation should stem from the balance between the rates of mass migration and cis-to-trans photoisomerization reaction. At the higher light intensities, the trans-isomers that induce the rigid liquid crystalline state is quickly accumulated before the mass transfer completes. On the other hand, when the intensities are too low, the transfer rate becomes too small that the surface tension will be shallow the SRG modulation.

From the above results, it is assumed that the migration process involves the following stages. Starting from the cis-rich photostationary state (fluid state), the  $\text{Ar}^+$  laser interference beam isomerizes the azobenzene units to the trans state. This

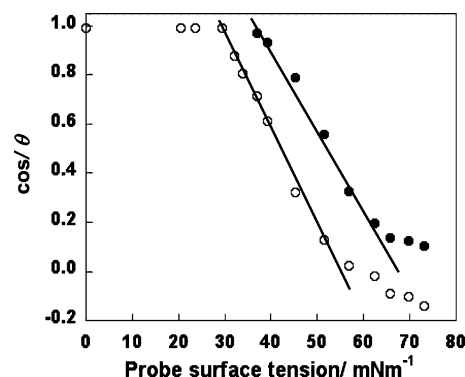


**Figure 5.** Cosine of contact angle  $\theta$  vs surface tension  $\gamma$  of probing liquid (Zisman plot) for the p6Az10Ac-PE4.5(50) film before (open circle) and after UV light irradiation. From these experiments, the critical surface energy,  $\gamma_c$ , for the *trans*-azobenzene film ( $\gamma_{c,trans}$ ) and cis-rich azobenzene film ( $\gamma_{c,cis}$ ) was estimated to be below 30 and 37  $\text{mN m}^{-1}$ , respectively.

spatial modulation in the population of trans/cis-isomers in the film brings about disparities and triggers the mass migration. When the film turns to the rigid liquid crystalline state, the cis content being lower than 40%, the morphology is fixed. Once the relief structure was formed, the undulated morphology could be stored without any change for more than 1 year at room temperature.<sup>17</sup> Probably, the local evolution of the liquid crystalline state imposes the deformation and migration of the neighboring regions in the isotropic state. In any case, the photochemical phase transition is strongly associated with both the initial mass migration and the subsequent fixation.

**Light-Modulated Critical Surface Tension.** We previously demonstrated that the highly efficient SRG formation observed in our polymer systems was promoted by the “intensity” holographic recording, independent of the polarization mode of light.<sup>16</sup> The polymer migration directs from the bright regions to dark ones under patterned nonpolarized blue light irradiation. Thus, the optical field gradient force, which has been frequently proposed to account for the mechanism of light-driven mass transport for amorphous azobenzene polymers, is not valid in the present system. The above results imply that the film deformation was predominately driven by self-assembling motions to minimize the free energy of the film system. Here, we consider another significant factor, the critical surface energy varied by the photochemical process.

Figure 5 indicates the Zisman plots (cosine of contact angle vs surface tension of the probing liquid) for nonirradiated and UV-irradiated thin films. The surface tension of the probing liquid was varied by the binary mixing of water and 1,4-dioxane with various proportions.<sup>21</sup> The contact angles were decreased after UV light irradiation.<sup>22,23</sup> The critical surface energy,  $\gamma_c$ , for the *trans*-azobenzene film ( $\gamma_{c,trans}$ ), derived from Young’s equation, was below 30  $\text{mN m}^{-1}$ , whereas that of the cis-rich state ( $\gamma_{c,cis}$ ) was 37  $\text{mN m}^{-1}$ . This significant change in critical surface energy can contribute to the evolution of the film deformation between the strongly illuminated region (trans-rich area) and weakly illuminated one (cis-rich area) in the micro-patterns. The photopatterned areas of different physical phases with different surface tensions can possibly promote plastic deformations at a micrometer scale in the time region of seconds. Nevertheless, further investigation is still required for the precise understanding.

**Photosensitized Isomerization and SRG Formation.** In amorphous films, repeated trans/cis isomerization during the illumination is supposed to be the essential driving force for the mass migration.<sup>9</sup> In contrast, as shown above, the occurrence

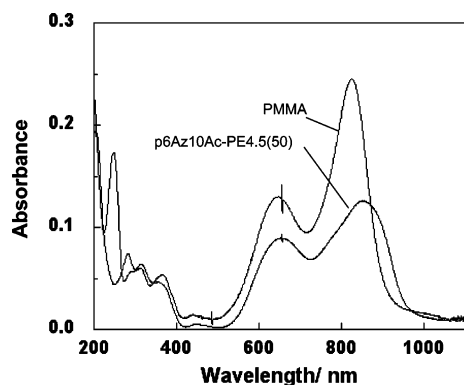


**Figure 6.** UV-vis absorption spectra of a near-infrared (IR) absorbing dye, polymethine dye IR820(B). The IR820(B) was dispersed into a PMMA or p6Az10Ac-PE4.5(50) thin film. The spectral feature of the PMMA film was in good agreement with that of THF solution.

of patterned photochemical phase transition accompanied by the one way *cis*-to-*trans* phase transition should be critical to the promotion of the markedly sensitive mass transfer phenomenon. In our system, the photon energy itself is not required for the mass transfer, but the change in the patterned photoinduced physical properties of the film plays the important role. Thus, it seemed of particular value to design an experiment by means of the *indirect* excitation of the *cis*-azobenzene, namely the sensitization from another dye molecule. If the system actually works, this can be clear evidence for our interpretation.

A binary mixed thin film containing both the azobenzene polymer and polymethine derivative, IR820(B), were prepared on a cleaned quartz substrate (Figure 6). As the control, the UV-vis absorption spectrum of IR820(B) dispersed in poly(methyl methacrylate) (PMMA) is also displayed. In PMMA a narrow absorption band at 820 nm in the near-infrared region was observed, which was in good agreement with that in THF solution. UV light illumination at 365 nm at a large amount of energy dose ( $10 \text{ J cm}^{-2}$ ) to this PMMA film did not change any spectral features. This fact ensures that IR820(B) molecule was photochemically stable and did not show bleaching within this exposure energy. In the p6Az10Ac-PE(50) film, the maximum wavelength showed a clear red shift from to 860 nm with some broadening, as shown in Figure 6. This spectral shift suggests the existence of the electronic interaction with the *trans*-azobenzene in the film.

Irradiation with UV light enhanced the absorption intensity at 440 nm assignable to the  $n\text{-}\pi^*$  band due to the *trans*-to-*cis* photoisomerization. At the same time, the absorption band around 840 nm enhanced concomitantly with an isosbestic point at 870 nm. Figure 7 shows the behaviors of the back reaction caused by the subsequent irradiation to the film with 436 nm (a), 633 nm (b), and near-infrared (810 nm) light (c). In all cases, the initial spectrum shown in Figure 6 was recovered. Of the three types of irradiation, only that with 436 nm light (a) corresponds to the direct excitation, and the remaining two are not absorbed by the *cis*-azobenzene. The *cis*-to-*trans* isomerization proceeded continuously in all cases regardless of the excitation wavelength, even though the *cis*-isomer was not directly excited for 633 and 810 nm irradiation. However, the isomerization rate strongly depended on the excitation wavelength. The direct excitation led to the fastest isomerization. For the two indirect excitations, the irradiation at 633 nm gave a much larger rate than that at 810 nm.

The time course of absorbance at 440 nm on the continuous exposure at 633 nm light is indicated in Figure 8. The absorption

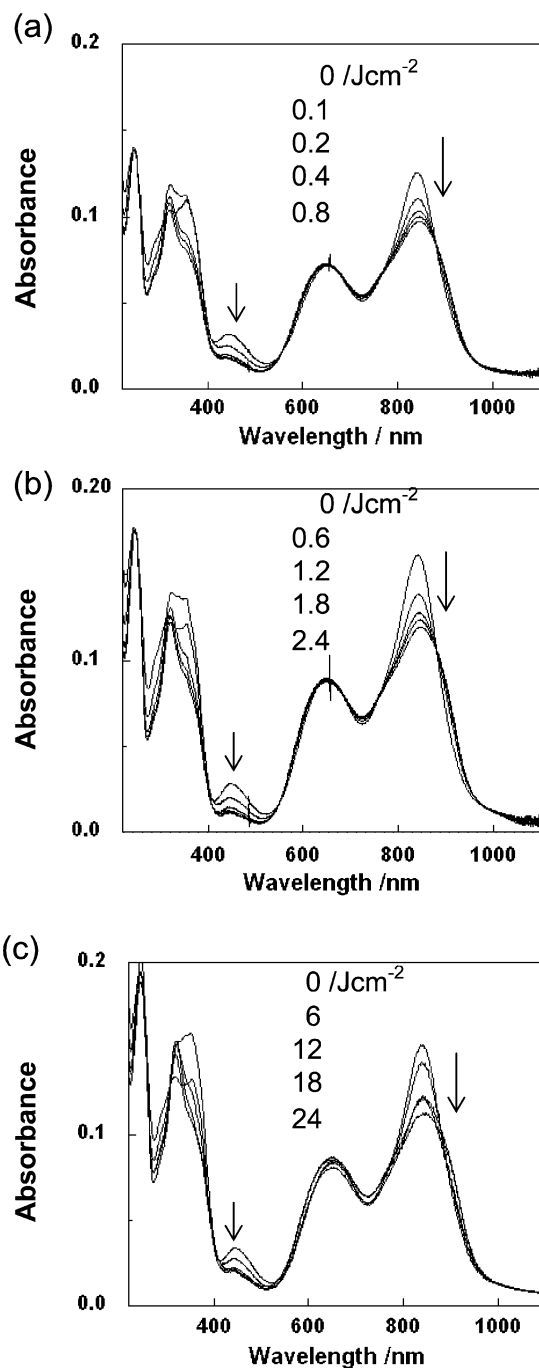


**Figure 7.** Spectral changes of the IR820(B)/*cis*-p6Az10Ac-PE4.5(50) films as a function of exposure energy of different excitation wavelengths: (a) 436 nm (direct excitation), (b) 633 nm (indirect excitation), and (c) 810 nm (indirect excitation).

intensity gradually decreased due to the *cis*-to-*trans* back-isomerization in both the absence and presence of the IR820(B). However, as clearly shown, the isomerization rate was accelerated in the presence of IR820(B) (open circles) compared with that without IR820(B) (closed circles). The reaction rate without IR820(B) under 633 nm irradiation was quite similar to that of the thermal back-isomerization at room temperature (closed squares), indicating that the *cis*-to-*trans* photoisomerization was not influenced by the illumination with He-Ne laser. These results show that, upon 633 nm excitation, the energy transfer from IR820(B) to the *cis*-isomer occurs and promotes the isomerization to the *trans*-form. Most probably, this sensitization occurs in the triplet state.<sup>24-27</sup>

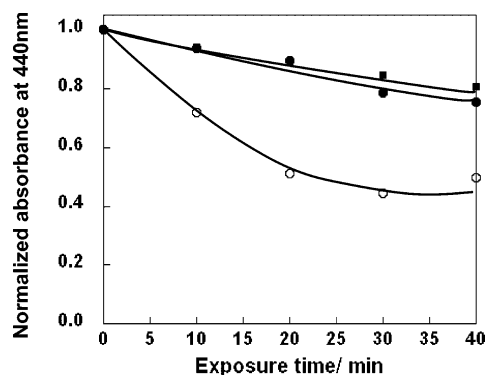


**Figure 8.** Changes in the normalized absorbance at 440 nm in cis-p6Az10Ac-PE4.5(50) films with time in the presence (open circle) and absence (closed circle) of IR820(B) in continuous irradiation at 633 nm at  $1.0 \text{ mW cm}^{-2}$ . As the control, data without irradiation are also shown with closed squares, which indicate the extent of thermal back-reaction at room temperature.

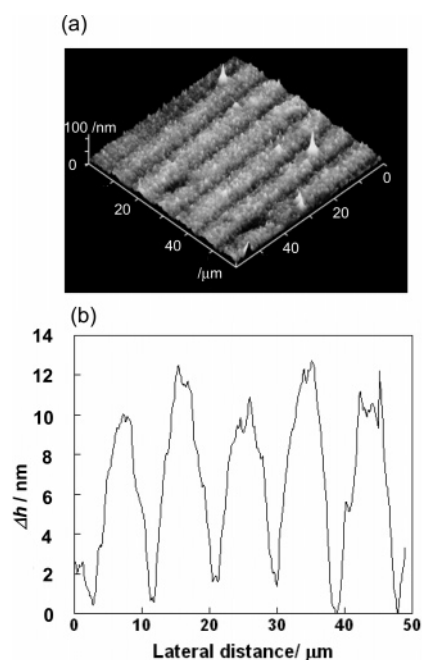


**Figure 9.** (a) Topographical AFM images and its cross-sectional profile of the undulation structure generated on a IR820(B)/p6Az10Ac-PE4.5-(50) film. The morphology was inscribed under irradiation with He–Ne laser (633 nm, via sensitization) at  $1.0 \text{ mW cm}^{-2}$  for 30 min.

Next, a question arises whether the sensitized excitation can lead to the mass transfer in the film. Here, a light amplitude pattern was attained with a line-space photomask with a period of  $4.0 \mu\text{m}$  windows. Irradiation with 633 nm light ( $1.0 \text{ mW cm}^{-2}$  for 30 min) was performed to the cis-rich film containing IR820(B). Figure 9 shows the topographic AFM image of the resulting film (a) and the cross-section profile (b). As shown, an undulated surface was obviously obtained following the mask pattern, indicating that the lateral material migration occurred via the sensitized isomerization. To our knowledge, this is the first observation of SRG formation via the sensitized excitation. Thus, the one-way isomerization from the cis to trans state actually induces the mass migration, and repeated back and forth isomerizations by the direct excitation process are not necessary. This result proves the significant aspect that the mass migration in the present system is started from the spatially patterned trans (liquid-crystalline state) and cis-rich (isotropic) areas.

## Conclusions

Use of liquid crystalline azobenzene polymer allows marked enhancement in the SRG formation upon patterned irradiation. The exact agreement of the cis-content value for the induction of the phase transition and the mass migration induction indicates that the photochemical phase transition plays the essential role in the mass migration. Also, the Zisman plot revealed that the photochemical phase transition leads to a significant change in the critical surface energy, which may possibly assist the mass migration. From the knowledge obtained here, the mechanism of the SRG formation in the present system is assumed as follows. The patterned irradiation gives rise to the spatial distributions of the trans-rich and cis-rich regions. The film material starts to move from the trans-rich regions to cis-rich ones, which is possibly initiated by the disparities of the viscosity and sharp gradient of surface tension at the boundary regions. The successful achievement of the relief formation via the sensitized excitation supports this interpretation. Here, the excitation at a much longer wavelength can induce the mass transfer of the azobenzene-containing film. This process overcomes the limitation of light source for excitation and expands the applicability of the light-generated relief formation. It is emphasized that the given photons are not used for the mass migration but only used to induce patterned physical properties in the film. Therefore, the present system should be recognized as a “phototriggered” process rather than a “photoinduced” one.

**Acknowledgment.** This work was supported by the Grant-in-Aid for Scientific Research (16205019) from the Ministry of Education, Culture, Sports, Science and Technology, Japan, CREST program of the Agency of Japan Science and Technology. N.Z. was partially supported by a research fellowship from the Japan Society for the Promotion of Science (JSPS).

## References and Notes

- (1) Natansohn, A.; Rochon, P. *Chem. Rev.* **2002**, *102*, 4139.
- (2) Ikeda, T. *J. Mater. Chem.* **2003**, *13*, 2037.
- (3) Ikeda, T.; Tsutsumi, O. *Science* **1995**, *268*, 1873.
- (4) Ichimura, K. *Chem. Rev.* **2000**, *100*, 1847.
- (5) Rochon, P.; Batalla, E.; Natansohn, A. *Appl. Phys. Lett.* **1995**, *66*, 136.
- (6) Kim, D.-Y. S.; Tripathy, K.; Li, L.; Kumar, J. *Appl. Phys. Lett.* **1995**, *66*, 1166.
- (7) Natansohn, A.; Rochon, P. *Adv. Mater.* **1999**, *11*, 1387.
- (8) Viswanathan, N. K.; Kim, D. Y.; Bian, S.; Williams, J.; Liu, W.; Li, L.; Samuelson, L.; Kumar, J.; Tripathy, S. K. *J. Mater. Chem.* **1999**, *9*, 1941.
- (9) Yager, K.; Barrett, C. *Curr. Opin. Solid State Mater. Sci.* **2001**, *5*, 487.
- (10) Ramanujam, P. S.; Holme, N. C. R.; Hvilsted, S. *Appl. Phys. Lett.* **1996**, *68*, 1329.
- (11) Hvilsted, S.; Ramanujam, P. S. *Monatsh. Chem.* **2001**, *132*, 43.
- (12) Gaididei, Y.; Christiansen, P.; Ramanujam, P. S. *Appl. Phys. B: Laser Opt.* **2002**, *74*, 139.
- (13) Yamamoto, T.; Hasegawa, M.; Kanazawa, A.; Shiono, T.; Ikeda, T. *J. Mater. Chem.* **2000**, *10*, 1493.
- (14) Pedersen, M.; Hvilsted, S.; Holme, N. C. R.; Ramanujam, P. S. *Macromol. Symp.* **1999**, *137*, 115.
- (15) Zettsu, N.; Ubukata, T.; Seki, T.; Ichimura, K. *Adv. Mater.* **2001**, *13*, 1693.
- (16) Zettsu, N.; Fukuda, T.; Matsuda, H.; Seki, T. *Appl. Phys. Lett.* **2003**, *83*, 4960.
- (17) Zettsu, N.; Seki, T. *Macromolecules* **2004**, *37*, 8692.
- (18) Ubukata, T.; Higuchi, T.; Zettsu, N.; Seki, T.; Hara, M. *Colloids Surf., A* **2005**, *257–258*, 123.
- (19) Ubukata, T.; Seki, T.; Ichimura, K. *Adv. Mater.* **2000**, *12*, 1675.
- (20) Tawa, K.; Zettsu, N.; Minematsu, K.; Ohta, K.; Namba, A.; Tran-Cong, Q. *J. Photochem. Photobiol. A* **2001**, *143*, 31.
- (21) Kabza, K.; Gestwich, J. E.; McGrath, J. L. *J. Chem. Educ.* **2000**, *77*, 63.

- (22) Oh, S.-K.; Nakagawa, M.; Ichimura, K. *J. Mater. Chem.* **2002**, *12*, 2262.
- (23) Ding, L.; Russel, T. P. *Macromolecules* **2007**, *40*, 2267.
- (24) Jones, L. B.; Hammond, G. S.; Saltiel, J.; Angelo, A.; Lamola, N. J.; Turro, J. S.; Bradshaw, D. O.; Cowan, R. C.; Ronald, C. *J. Am. Chem. Soc.* **1965**, *87*, 4219.
- (25) Malkin, S.; Fisger, E. *J. Phys. Chem.* **1964**, *68*, 1153.
- (26) Hammond, G. S.; Saltiel, J.; Lamola, A. A.; Turro, N. J.; Bradshaw, J. S.; Cowan, D. O.; Counsell, R. C.; Vogt, V.; Dalton, C. *J. Am. Chem. Soc.* **1964**, *86*, 3197.
- (27) Fischer, E. *J. Am. Chem. Soc.* **1968**, *90*, 796.

MA0706428